J. Phys. Chem. A **1998,** *102,* 10493−10500

The Mechanism of the Gas-Phase Ion−Molecule Reaction between Al$^+$ and Ethanol

Detlef Stöckigt[†]

Abteilung Massenspektrometrie, Max-Planck-Institut für Kohlenforschung, Kaiser-Wilhelm-Platz 1,
D-45470 Mülheim an der Ruhr, Germany

Received: May 6, 1998; In Final Form: August 26, 1998

The reaction between a ground-state aluminum cation and a single ethanol molecule has been investigated by computational chemistry. The structures and relative energies of reactants, intermediates, products, and transition states have been examined employing density functional theory (DFT) methods. The data are compared to those from Hartree−Fock (HF), Møller−Plesset perturbation (MP), and Gaussian [G1, G2, G2(MP2), G2(QCI)] calculations. According to recent gas-phase experiments, the low-energy collision between Al$^+$ and ethanol results solely in the formation of Al(H$_2$O)$^+$ and ethylene. The present study confirms that Al$^+$ (^{1}S) and ethanol react to yield Al(H$_2$O)$^+$ and ethylene as the dominant products at thermal energies. Three different reaction paths have been considered, among them, an oxidative-addition and reductive-elimination mechanism. The reaction proceeds via an aluminum-cation-catalyzed, one-step syn elimination with a cyclic transition state. The relative energy of this transition state is *similar to or below* that of the entrance channel and lower than that of the highest of the other pathways. On the basis of these results, a new elimination reaction mechanism is introduced: Induced by an *electrophile*, one-step syn elimination takes place via a cyclic transition state following a second-order kinetic (E_{E2}) mechanism.

1. Introduction

In homo- and heterogeneous catalysis, most of the bond-making and -breaking processes occur at coordinatively unsaturated metal centers, e.g., electron-deficient aluminum complexes.[1] For the development of industrial applications, a more direct structure-to-reactivity relationship is highly desirable for these "cation-like" catalytic centers.[2] Additionally, detailed knowledge of underlying reaction mechanisms facilitates the improvement of stereo- and enantioselectivity. One scientific approach toward elucidating such processes is based on the exclusion of secondary influences (for example, counterions, solvent composition, temperature, and concentration) and, hence, focuses on the respective gas-phase potential-energy surface (PES).

Studying the *interacting forces* among metal cations and small organic ligands can be achieved by several mass spectrometry-related experiments, among them, bracketing,[3] infrared radiative cooling,[4] photodissociation,[5] and threshold collision-induced dissociation.[6] The most accurate bond-dissociation energies of M$^+$−L complexes (M, metal atom; L, ligand), however, have been obtained by vibrationally resolved photodissociation spectra.[7] Concerning Al$^+$−L bond-dissociation energies and enthalpies,[8] the early reports on ligand-exchange equilibrium measurements[9] from Uppal and Staley[10a] and from the group of McIver[10b] still represent valuable sources. To outline the *mechanism* of ion−molecule reactions, matrix isolation,[11] mass spectrometry,[12] or quantum chemistry[13−15] can be employed. These techniques enable the observation, manipulation or characterization of selected species which are otherwise not easily accessible.

The aim of the present work is to study the gas-phase reaction between Al$^+$ (^{1}S) and ethanol by employing density functional theory (DFT). As observed by Uppal and Staley[10a] and confirmed by Chowdhury and Wilkins,[16] Al(H$_2$O)$^+$ and ethylene are formed solely in the gas-phase reaction between the aluminum cation and ethanol (eqs 1 and 2). The collision

$$\mathrm{Al^+ + C_2H_5OH \rightarrow Al(C_2H_5OH)^+} \quad (1)$$

$$\mathrm{Al(C_2H_5OH)^+ \rightarrow Al(H_2O)^+ + C_2H_4} \quad (2)$$

complex, Al(C$_2$H$_5$OH)$^+$ in eq 1, has not been detected because of its short lifetime. However, Al(C$_2$H$_5$OH)$^+$ is a secondary reaction product due to ligand exchange. Experiments on selectively deuterium-labeled Al$^+$−ethanol systems provided evidence that ethylene expulsion occurs without H/D scrambling (eq 3).[16b] Recently, the groups of Ohanessian and McMahon

$$\mathrm{Al^+ + CD_3CH_2OH \rightarrow Al(HDO)^+ + CD_2{=}CH_2} \quad (3)$$

supported these early findings by studying the reaction under high-pressure conditions.[17] They suggested the involvement of the oxidative insertion of an aluminum ion into the HO−C$_2$H$_5$ bond as a possible commencing reaction step for the process in eq 2, in contrast to previous assumptions.[10a,16]

In this contribution, reaction mechanisms[18] for the elementary gas-phase process depicted in eq 2 will be discussed on the basis of DFT results. Three different reaction pathways will be considered for the ethylene expulsion according to eq 2: (i) oxidative addition, β-H shift, and reductive elimination, (ii) oxidative addition followed by a 1,4-hydrogen transfer to yield (H$_2$O)Al(C$_2$H$_4$)$^+$, and (iii) one-step syn elimination. The first one is known for late-transition-metal chemistry (Scheme 1),[19] occurring, for example, in the Heck reaction.[20] The third one is related to the dissociation of protonated ethanol (Scheme 2)[21] or the ion/dipole mechanism proposed by Eller and Schwarz (Scheme 3).[22] The *interacting forces* in Al$^+$−L complexes[8b] are expected to play principally an intermediate role between (i) the dominant covalent-binding character in multiplet transition-

---

[†] E-mail: stoeckigt@mpi-muelheim.mpg.de.

10.1021/jp982139q CCC: $15.00

SCHEME 1

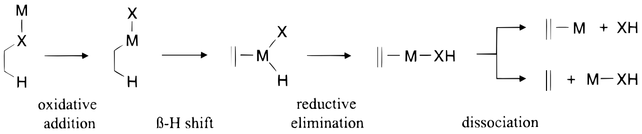

M: transition metal, e.g. Pd X: functional group, e.g. I or AcO

SCHEME 2

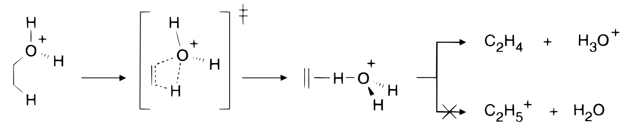

SCHEME 3

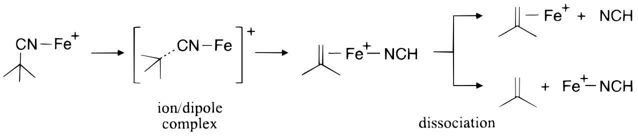

metal ion complexes[23] and (ii) the mainly electrostatic interaction of singlet-state alkali ions (or a proton) with ligands because of the polarizable $3s^2$ shell of Al^+ (^1S).[24]

2. Computational Details

The calculations have been performed by using the Gaussian 94 program package[25] within the DFT framework[26] according to Kohn and Sham.[27] Digital DEC 3000/300 workstations and a SGI Power Challenge R8000 with four processors have been applied. Taking advantage of the gradient-corrected local density approximation,[28,29] the exchange functional by Becke (B)[29f] and the correlation functionals reported by Lee, Yang, and Parr (LYP)[29d] and by Perdew and Wang (PW91)[29g] have been utilized. In addition, Becke has suggested[29i] the admixing of a fraction of the exact Hartree−Fock (HF) exchange, thus resulting in a DFT/HF hybrid functional. Compared with pure density functionals, it was significantly more accurate with regard to the atomization energies and ionization potentials of 56 Gaussian-2 (G2)[30] molecules.[31] Related hybrid functionals (B3LYP and B3PW91) have been utilized in the present work, as implemented by Gaussian, Inc.[25,32] Geometries of reactants, transition states, and products were fully optimized. If a higher symmetry point group than C_1 resulted from the optimization, the respective constraints were introduced, and the calculations were repeated.

According to previous suggestions,[8,33,34] basis-set requirements are much less stringent for DFT than for post-HF methods. Pople's split-valence basis sets including polarization and diffuse functions ("6-31G(d)", "6-311+G(d)", and "6-311++G(3df,2p)")[35] and the correlation-consistent basis sets "cc-pVDZ" and "cc-pVTZ" reported from the group of Dunning[36] have been used.[25,37] The zero-point vibrational energies (ZPVE) as obtained from the respective methods have been scaled by 0.98 (DFT, DFT/HF), 0.86 (HF), and 0.96 (MP2). The reported energies result from the ZPVE-corrected B3PW91/6-311++G(3df,2p)//B3PW91/6-311+G(d) method unless otherwise stated. The imaginary frequencies are quoted from the B3PW91/6-311+G(d) level of theory without scaling.[38] The minimum-energy pathway from transition states toward reactants and products has been calculated by applying intrinsic reaction coordinate (IRC) calculations.[39]

Theoretical methods employed here also involved second-order Møller−Plesset perturbational theory with all electrons correlated (MP2)[40] and the Gaussian approach abbreviated G1, G2, G2(MP2), and G2(QCI).[30,41] In our previous investigations on ground-state $Al(L)^+$ complexes,[8] the agreement between DFT-calculated and experimental relative energies turned out to be satisfactory. DFT- and DFT/HF-calculated bond-dissociation energies $D_0(Al^+{-}L)$ and the relative energies of $Al(L^1)^+$ vs $Al(L^2)^+$ complexes result in data with an accuracy of better than ±5 kcal/mol.[8,32,42] The structural parameters of the $Al(L)^+$ complexes obtained by DFT are expected to be accompanied with an accuracy of better than ±0.1 Å for bond lengths and ±5° for bond angles. DFT has also been tested[43] and applied[44] for the prediction of transition states' geometries and energies. However, in comparison with HF, MP2, G2, and experimental data, the relative energies of reaction barriers are sometimes underestimated by density functional approximations.[43]

3. Results and Discussion

The computed absolute energies and selected geometrical data [BPW91/6-311+G(d)][45] for stationary points of the $[Al^+,C_2H_5OH]$ PES are presented in Table 1 and Figure 1, respectively. The computed results for several $Al(C_2H_5OH)^+$ complexes (**1**) are discussed in section 3.1. The following sections deal with (3.2) the oxidative-addition, β-H shift, and reductive-elimination pathway; (3.3) a mechanism commencing with oxidative addition and followed by a 1,4-H shift, and (3.4) the one-step syn-elimination pathway. In section 3.5, the data obtained with different computational methods will be compared in more detail. The introduction of the E_{E2} concept (3.6) closes this section. Considering the experimental results given in eq 3, an Al^+-induced 1,1-elimination of H_2O from ethanol can be ruled out in the given system. The formation of Al(OH) and $C_2H_5^+$ has been calculated to be endothermic by 10.5 kcal/mol. They have not been considered further.

3.1. Gas-Phase $Al(C_2H_5OH)^+$ Complexes. The (C−C−O−H) anti conformer of ethanol is known to be about 0.3−0.5 kcal/mol more stable than the gauche conformer in the gas phase.[46a] As reported previously[46b] and confirmed here, the results of the HF, MP2, and DFT methods yield the correct energetic ordering of the gauche vs anti conformer depending on the applied basis set. Utilization of the Gaussian methods, however, leads to the correct result only for G2(QCI): At 0 K, the gauche conformer is computed to be more stable by 0.2 kcal/mol (G1), 0.1 kcal/mol (G2), and 0.1 kcal/mol [G2(MP2)]. Within the methods' limits of accuracy, however, all of the calculated data agree with the experimental ones (Table 2).

The following isomers and conformers of the $Al(C_2H_5OH)^+$ complex (**1**) have been detected. Al^+ is coordinated to the oxygen atom of the anti conformer of ethanol in **1a** (C_s). In **1b** (C_1), Al^+ is attached to the oxygen atom of the gauche conformer. In other respects, the geometrical parameters of **1a** and **1b** are similar considering the applied methods.[45b] The calculated relative energies of these complexes are presented in Table 2. On the basis of the ligand-exchange experiments at 298 K, $\Delta H_{diss}(Al^+{-}C_2H_5OH)$ was determined to be 36.6[10a] and 36.4 kcal/mol.[10b] The B3PW91 calculated $D_0(Al^+{-}C_2H_5OH)$ was determined to be 35.6 kcal/mol (**1a**) and 36.2 kcal/mol (**1b**). The G2-calculated $\Delta H_{diss}(Al^+{-}C_2H_5OH)$ at 298 K was determined to be 36.4 (**1a**) and 36.9 kcal/mol (**1b**). As an estimate for the basis-set superposition error, the counterpoise correction has been computed to be less than 1.0 kcal/mol for **1a** and **1b** with the DFT and G2 methods. A rotational barrier[47] of ca. 1−2 kcal/mol connects **1a** and **1b**. Therefore, the role of the conformers **1a** and **1b** can be considered equivalent concerning the reaction mechanisms underlying eq 2.

TABLE 1: Absolute Energies (Hartrees) of Stationary Points of the [Al^+,C_2H_5OH] PES As Obtained with the Indicated Quantum Chemical Methods Including ZPVE Values

species	HF[a]	MP2[b]	G1	G2	G2(MP2)	G2(QCI)	BPW91[a]	B3PW91[a]	B3LYP[a]
Al^+	−241.668 021	−241.820 650	−241.713 786	−241.713 030	−241.713 810	−241.712 848	−242.142 818	−242.106 387	−242.165 422
$C_2H_5OH_{anti}$	−154.065 898	−154.575 906	−154.758 983	−154.764 463	−154.760 512	−154.762 781	−155.007 630	−154.972 397	−155.034 158
$C_2H_5OH_{gauche}$	−154.065 532	−154.575 592	−154.758 642	−154.764 273	−154.760 321	−154.762 619	−155.007 628	−154.972 316	−155.033 966
$Al(C_2H_5OH)^+$ (**1a**)	−395.783 124	−396.531 033	−396.532 433	−396.534 861	−396.531 327	−396.533 019	−397.199 825	−397.128 244	−397.327 461
$Al(C_2H_5OH)^+$ (**1b**)	−395.784 682	−396.531 913	−396.532 932	−396.535 597	−396.530 287	−396.533 799	−397.201 672	−397.129 341	−397.328 777
TS 1/2	−395.726 156	−396.457 076	−396.476 564	−396.477 758	−396.473 548	−396.475 415	−397.158 900	−397.078 336	−397.274 419
$C_2H_5{-}Al^+{-}OH$ (**2**)	−395.802 443	−396.547 374	−396.552 962	−396.556 938	−396.552 145	−396.555 206	−397.225 441	−397.153 776	−397.346 205
TS 2/3	−395.747 165	−396.474 747	−396.495 004	−396.497 914	−396.492 815	−396.496 214	−397.172 231[c]	−397.099 190[c]	−397.285 947
$(C_2H_4)Al^+(H)(OH)$ (**3**)	−395.796 868	−396.526 453	−396.543 967	−396.545 339	−396.540 064	−396.543 295	−397.210 656	−397.138 523	−397.329 596
TS 3/4	−395.659 560	−396.414 682[c]	−396.439 494	−396.440 623	−396.436 434	−396.438 241	−397.125 968	−397.041 911	−397.228 661
$(C_2H_4)Al^+(H_2O)$ (**4a**)	−395.768 120	−396.507 377	−396.516 810	−396.519 246	−396.515 567	−396.517 300	−397.187 679	−397.112 742	−397.311 260
$(C_2H_4)Al^+(H_2O)$ (**4b**)	−395.765 267	−396.503 848	−396.514 417	−396.516 894	−396.513 096	−396.514 908	−397.185 992	−397.110 749	−397.307 623
TS 2/4	−395.723 902	−396.450 768	−396.469 028	−396.469 593	−396.464 923	−396.467 480	−397.150 611	−397.071 591	−397.192 975
TS 1/4	−395.731 638	−396.461 858	−396.477 602	−396.477 669	−396.473 514	−396.475 446	−397.150 420	−397.073 565	−397.268 481
$Al(H_2O)^+$	−317.741 796	−318.114 661	−318.086 238	−318.086 645	−318.084 900	−318.085 933	−318.621 117	−318.560 931	−318.651 360
C_2H_4	−78.014 578	−78.307 021	−78.414 006	−78.415 928	−78.414 296	−78.414 659	−78.556 982	−78.535 728	−78.575 935
$Al(C_2H_4)^+$	−319.699 368	−320.148 447	−320.149 586	−320.150 540	−320.149 259	−320.149 144	−320.725 629	−320.666 906	−320.763 197
H_2O	−76.037 663	−76.244 402	−76.328 338	−76.332 051	−76.330 008	−76.331 231	−76.436 093	−76.412 006	−76.444 396

[a] Basis set: 6-311++G(3df,2p). [b] MP2(full)/6-311+G(d), with MP2(full)/6-31G(d) zero-point vibrational energies scaled by 0.94. [c] Another conformer with a similar energy (less than 5 ppm difference) was found.

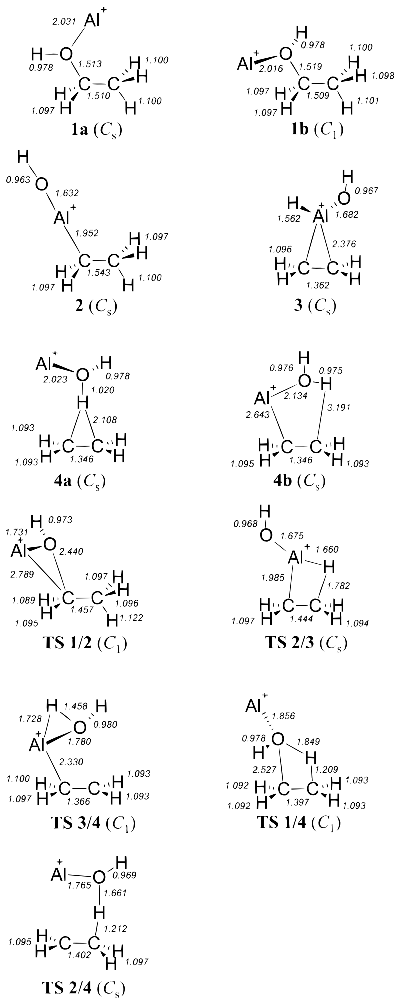

Figure 1. Geometrical data of stationary points of the [Al^+,C_2H_5OH] PES. The data were obtained from the BPW91/6-311+G(d) level of theory.

Two additional $Al(C_2H_5OH)^+$ isomers have been discovered. In **1c** (C_s), the ethanol ligand is η^3-coordinated to Al^+ via the three hydrogen atoms of the terminal CH_3 group of ethanol. In **1d** (C_s), aluminum interacts with one hydrogen atom of the terminal CH_3 group of ethanol and the two equivalent hydrogen atoms of the $CH_2(OH)$ group. The relative energies of the latter two isomers, however, amount to ca. −5 to −10 kcal/mol (data not shown). These relative energies are higher than those of the isomers **1a** and **1b** by at least 25 kcal/mol. The barriers for the transformation **1c** $\rightleftharpoons$ **1d** and **1c** or **1d** → **1a** and **1b** are below 5 kcal/mol. Once formed from Al^+ and ethanol, the isomers **1c** and **1d** will subsequently convert to **1a** or **1b** under thermal conditions. Therefore, **1c** and **1d** will not be further examined with regard to the gas-phase process depicted in eq 2.

3.2. Oxidative-Addition, β-H Shift, and Reductive-Elimination Pathway. With respect to the reaction between a late transition-metal complex and ethanol, the classical oxidative-addition, β-H shift, and reductive-elimination reaction mechanisms analogous to Scheme 1 (X = OH; R = H) can be expected. The corresponding pathway for the Al^+ + ethanol process will be described in this section on the basis of DFT-computed data.

As shown in Scheme 4 and in Figure 2, the first step of the reaction of Al^+ + ethanol yields an $Al(C_2H_5OH)^+$ complex (**1a** or **1b**, cf. section 3.1 and eq 1). According to IRC calculations, the oxidative addition of ethanol to the aluminum cation center

TABLE 2: Relative Energies (kcal/mol) of Stationary Points of the [Al^+,C_2H_5OH] PES As Obtained with the Indicated Quantum Chemical Methods Including ZPVE Values

species	HF[a]	MP2[b]	G1	G2	G2(MP2)	G2(QCI)	BPW91[a]	B3PW91[a]	B3LYP[a]
$Al^+ + C_2H_5OH_{anti}$	0.0	0.0	0.0	0.0	0.0	0.0	0.0	0.0	0.0
$Al^+ + C_2H_5OH_{gauche}$	0.2	0.2	−0.2	−0.1	−0.1	0.1	0.0	0.1	0.1
$Al(C_2H_5OH)^+$ (**1a**)	−30.9	−38.5	−37.4	−36.0	−35.8	−36.0	−35.4	−35.6	−34.6
$Al(C_2H_5OH)^+$ (**1b**)	−31.9	−39.0	−37.8	−36.5	−35.1	−36.5	−36.5	−36.2	−35.6
TS 1/2	4.9	7.9	−2.4	−0.2	0.5	0.1	−9.7	−4.2	−4.9
$C_2H_5{-}Al^+{-}OH$ (**2**)	−43.0	−48.8	−50.3	−49.9	−48.8	−49.9	−51.5	−51.6	−48.4
TS 2/3	−8.3	−3.2	−14.0	−12.8	−11.6	−12.9	−18.1[c]	−17.3[c]	−13.5
$(C_2H_4)Al^+(H)(OH)$ (**3**)	−39.5	−35.6	−44.7	−42.6	−41.3	−42.5	−42.2	−42.0	−40.7
TS 3/4	46.7	34.5[c]	20.9	23.1	23.8	23.5	11.0	18.6	20.1
$(C_2H_4)Al^+(H_2O)$ (**4a**)	−21.5	−23.7	−27.6	−26.2	−25.9	−26.1	−27.8	−25.8	−27.4
$(C_2H_4)Al^+(H_2O)$ (**4b**)	−19.7	−21.4	−26.1	−24.7	−24.3	−24.6	−26.7	−24.6	−25.1
TS 2/4	6.3	11.9	2.3	5.0	5.9	5.1	−4.5	0.0	−0.4
TS 1/4	1.4	4.9	−3.0	−0.1	0.5	0.1	−4.4	−1.2	−2.3
$Al(H_2O)^+ + C_2H_4$	−14.1	−12.1	−17.2	−15.7	−15.6	−15.8	−17.6	−15.7	−17.7
$Al(C_2H4)^+ + H_2O$	−2.0	6.5	−3.2	−3.2	−3.1	−3.2	−7.4	−4.6	−5.4
$Al^+ + H_2O + C_2H_4$	12.9	20.2	10.4	10.3	10.2	10.6	8.7	11.0	8.2

[a] Basis set: 6-311++G(3df,2p). [b] MP2(full)/6-311+G(d), with MP2(full)/6-31G(d) zero-point vibrational energies scaled by 0.94. [c] Another conformer with a similar energy (less than 5% difference) was found.

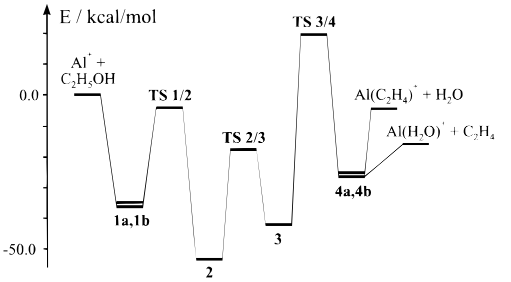

Figure 2. Schematic drawing of the PES for the oxidative-addition and reductive-elimination pathway in the reaction of Al^+ (^1S) + C_2H_5OH. The data were calculated with the B3PW91/6-311++G(3df,2p)//B3PW91/6-311+G(d) method (cf. Table 2 and Scheme 4; *E* = relative energy).

SCHEME 4

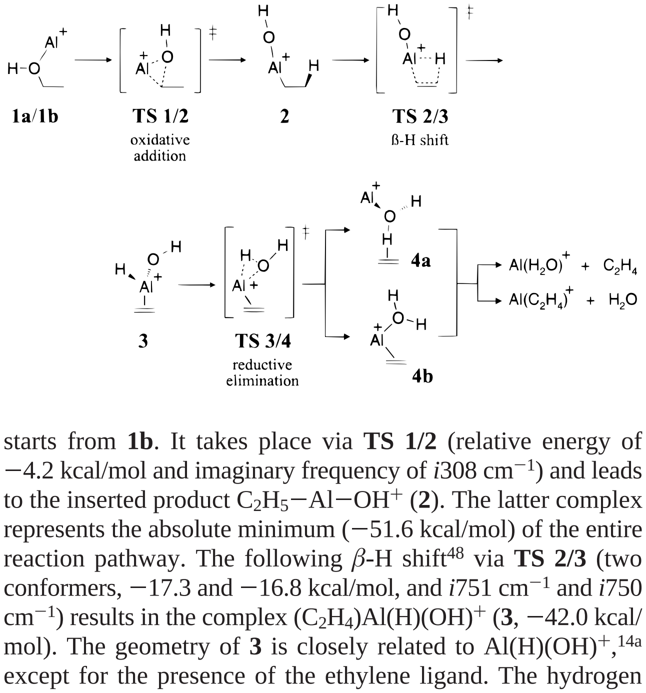

starts from **1b**. It takes place via **TS 1/2** (relative energy of −4.2 kcal/mol and imaginary frequency of *i*308 cm^{-1}) and leads to the inserted product $C_2H_5{-}Al{-}OH^+$ (**2**). The latter complex represents the absolute minimum (−51.6 kcal/mol) of the entire reaction pathway. The following β-H shift[48] via **TS 2/3** (two conformers, −17.3 and −16.8 kcal/mol, and *i*751 cm^{-1} and *i*750 cm^{-1}) results in the complex $(C_2H_4)Al(H)(OH)^+$ (**3**, −42.0 kcal/mol). The geometry of **3** is closely related to $Al(H)(OH)^+$,[14a] except for the presence of the ethylene ligand. The hydrogen migration from Al^+ in **3** to the oxygen atom can be termed a reductive-elimination step via **TS 3/4** (+18.6 kcal/mol, *i*1358 cm^{-1}), yielding two $(C_2H_4)Al(H_2O)^+$ species: **4a** (−25.8 kcal/mol) and **4b** (−24.6 kcal/mol). A small energy barrier separates the isomers **4a** and **4b** (−26.0 kcal/mol, *i*21 cm^{-1}). In addition, the barrier for the water rotation along the Al−O axis in **4b** (−25.8 kcal/mol, *i*150 cm^{-1}) enables switching of the water hydrogens. Again, the geometry of the $Al(H_2O)^+$ moiety in **4a** and **4b** is very similar to that of free $Al(H_2O)^+$.[8a,14]

The barrier height for the reductive-elimination process **3** → **4** is above the dissociation limit and, therefore, inaccessible for the system under thermal conditions. This height can be rationalized in terms of the analysis used by Siegbahn et al.[49] From left to right, the processes given in eqs 4−6 represent reductive-elimination steps of X−OH from $X{-}Al^+{-}OH$ with X = H, R in (i) the "naked" systems [Al^+,H_2O] (eq 4a),[14a,15h] [Al^+,CH_3OH] (eq 4b), and [Al^+,C_2H_5OH] (eq 4c, i.e., **2** → **1**) and (ii) a system containing an additional ligand π bonded to the aluminum center (eq 5, i.e., **3** → **4**):

$$H{-}Al^+{-}OH \rightarrow Al(H_2O)^+ \tag{4a}$$

$$CH_3{-}Al^+{-}OH \rightarrow Al(CH_3OH)^+ \tag{4b}$$

$$C_2H_5{-}Al^+{-}OH \rightarrow Al(C_2H_5OH)^+ \tag{4c}$$

$$(\pi\text{-L})Al(H)(OH)^+ \rightarrow (\pi\text{-L})Al(H_2O)^+ \quad (\pi\text{-L} = C_2H_4) \tag{5}$$

In the simple system of eq 4a, the height of the reaction barrier was calculated to be 56.0[15h] and 55.2 kcal/mol.[14a] The relative energy of the transition state belonging to eq 4b is ca. 62.6 kcal/mol[50] above that of $CH_3{-}Al^+{-}OH$. The barrier height for the process **2** → **1** (eq 4c) is 47.4 kcal/mol (Table 2). Equations 4a−c have in common the following: (i) a mixing of s and p states in Al^+ [Ne]$3s^2$ is energetically too demanding and (ii) the $3s^2$ configuration prevents strong bond formation and close approach of the ligand because of Pauli repulsion.[49] Following Siegbahn et al.,[49] the Al^+ [Ne]$3s^2$ interaction with Y−H bonds (Y = HO,[14a] H_2N, H_3C, NC,[14c] and CN,[14c] CCH[14b]) can be termed ineffective, and high barriers have been found for the reductive elimination of Y−H.

The conversion **3** → **4** is given in eq 5. Compared with the naked [Al^+,H_2O] system of eq 4a, a π-L has been added in **3** and **4**, but a severe change of the electron configuration of Al in **3** and **4** does not occur. Low-lying s or p states of Al^+ in **3** and **4** are not present. Therefore, a barrier height of 53.2 kcal/mol results for $(\pi\text{-L})Al(H)(OH)^+ \rightarrow (\pi\text{-L})Al(H_2O)^+$, similar to that of the naked [Al^+,H_2O] system (63.8 kcal/mol).[14a]

3.3. Oxidative Addition followed by a 1,4-H Shift. The oxidative addition of ethanol to a ground-state aluminum cation

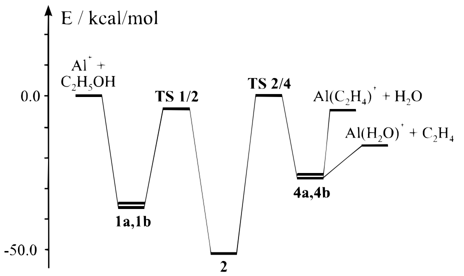

Figure 3. Schematic drawing of the PES for the oxidative addition and 1,4-H shift pathway in the reaction of Al^+ (^1S) + C_2H_5OH. The data were calculated with the B3PW91/6-311++G(3df,2p)//B3PW91/6-311+G(d) method (cf. Table 2 and Scheme 5; E = relative energy).

SCHEME 5

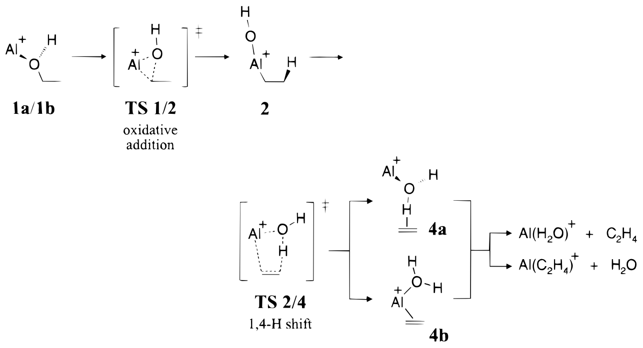

proceeds via **TS 1/2** (Scheme 4). It has been shown to be energetically less demanding (DFT and DFT/HF) or similar (G2) to the dissociation limit in the previous section (3.2). Because the relative energy of the barrier for the reductive elimination (**TS 3/4**, Scheme 4) is clearly above the dissociation limit, process **3** → **4** is inaccessible under thermal conditions. However, there exists an alternative reaction pathway circumventing **TS 3/4**: a 1,4-H shift from **2** to **4a**/**4b**.

From the aluminum complex $C_2H_5-Al^+-OH$ (**2**), a cyclic transition state for a 1,4-H shift (**TS 2/4**) leads directly to the product complexes **4a** or **4b** (Scheme 5). The relative energy of **TS 2/4** is above the dissociation limit by 6.3, 11.9, 2.3, 5.0, 5.9, and 5.1 kcal/mol, if one takes the data from the HF, MP2, G1, G2, G2(MP2), and G2(QCI) calculations into account, respectively. In contrast, the DFT methods predict this barrier height to be −4.5 (BPW91), −0.4 (B3LYP) and 0.0 kcal/mol (B3PW91) (Figure 3). Notably, the barrier height for **2** → **4** is considerably below that of the reductive oxidation step **3** → **4** (18.6 kcal/mol) as discussed in section 3.2. Nevertheless, the reaction sequence **1** → **2** → **4** passes through two transition states which are both close to the dissociation limit.

3.4. One-Step Syn-Elimination Pathway. Ethylene and a hydronium ion have been reported as exothermic products in a one-step reaction via a single TS (Scheme 2) for the protonation reaction of ethanol.[21] The formation of an ethyl cation and water turned out to be endothermic.[21] A respective one-step syn-elimination pathway for the Al^+ + ethanol system will be outlined in this section (Scheme 6).

The addition of the singlet-state aluminum cation to ethanol leads barrierless to the already discussed complexes **1a** or **1b**. According to IRC calculations, the transition state **TS 1/4** (i679 cm^{-1}) connects **1b** *directly* with **4a**. This process can be considered an electrophile-induced syn-elimination reaction with a cyclic transition state. The respective barrier height is −1.2 kcal/mol (Figure 4), which is energetically close to or below the dissociation limit (Table 2). The product **4a** (−25.8 kcal/mol) is formed without any intermediate. Because of the small barriers, **4a** can easily convert to **4b** and vice versa (for more details on this part of the PES, see section 3.2). The subsequent expulsion of neutral water or ethylene from **4a** or **4b** can yield $Al(C_2H_4)^+$ (−4.6 kcal/mol) or $Al(H_2O)^+$ (−15.7 kcal/mol), respectively. An additional transition state has not been detected in any of these cases. Therefore, the relative energies of the exit channels reflect the heights of the reaction barriers,[51] and $Al(H_2O)^+$ is expected to be the major product in the reaction of Al^+ and ethanol. This finding is in line with the experimental results.[10a,16,17] The decisive rate-determining step for the overall reaction according to eq 2 appears to be passing **TS 1/4**.

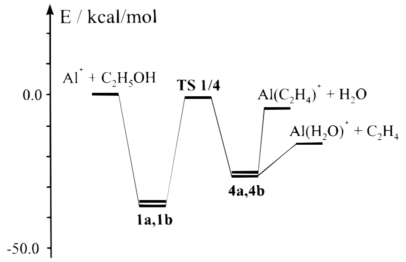

Figure 4. Schematic drawing of the PES for the one-step syn-elimination pathway in the reaction of Al^+ (^1S) + C_2H_5OH. The data were calculated with the B3PW91/6-311++G(3df,2p)//B3PW91/6-311+G(d) method (cf. Table 2 and Scheme 6; E = relative energy).

SCHEME 6

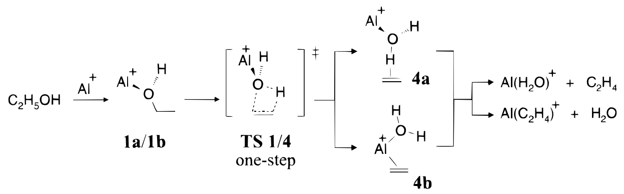

3.5. Discussion of DFT Data. Compared to the G2 data, the BPW91-, B3PW91-, or B3LYP-computed bond-dissociation energies (D_0) of several Al^+-L complexes have been predicted to within ±5 kcal/mol, if basis sets of at least double-ζ quality were applied.[8] On the basis of the results of the present study, a similar conclusion can be drawn (cf. Tables 2 and 3). With regard to the minima of the $[Al^+,C_2H_5OH]$ PES, the relative energies calculated by DFT or DFT/HF-hybrid methods coincide with the G2 data within ±2 kcal/mol if basis sets of at least double-ζ quality have been used. Compared to those of the B3LYP-based data, the relative energies obtained by BPW91 and B3PW91 result in slightly lower values (1−3 kcal/mol) for all tested basis sets.[52] The best agreement with the G2 data is obtained by using B3PW91/6-311++G(3df,2p), i.e., better than ±2 kcal/mol. In addition, cc-pVTZ performs very well, followed by 6-311+G(d), cc-pVDZ, and 6-31G(d). Even in the latter case, the averaged difference to the G2 data is only ca. ±4 kcal/mol (Table 3, except for the last entry).

An inaccuracy has to be noted in the BPW91-computed exit channel $Al(C_2H_4)^+ + H_2O$. The 6-311++G(3df,2p)-calculated relative energy is −7.4 kcal/mol whereas the G2 value is −3.2 kcal/mol (−4.6 kcal/mol for B3PW91 and −5.4 kcal/mol for B3LYP; for the cc-pVTZ basis set, a similar trend has been observed; the BPW91 counterpoise correction is −0.4 kcal/mol), i.e., a difference between G2 and BPW91 of 4.2 kcal/mol. The following explanation for this discrepancy is presented. $D_0(Al^+-C_2H_4)$ = 13.6 kcal/mol has been computed,[3d] the present G2 value is 13.5 kcal/mol, and Kemper et al. measured 14.9 kcal/mol recently.[24c] The BPW91 result, however, is 16.1

TABLE 3: Relative Energies (kcal/mol) of Stationary Points of the [Al^+,C_2H_5OH] PES as Calculated with G2, B3LYP, BPW91, and B3PW91 Methods Including ZPVE Values and Depending on Selected Basis Sets

		6-311++G(3df,2p)			6-311+G(d)			6-31G(d)		cc-pVTZ		cc-pVDZ	
species	G2	B3LYP	BPW91	B3PW91	B3LYP	BPW91	B3PW91	B3LYP	BPW91	B3LYP	BPW91	B3LYP	B3PW91
$Al^+ + C_2H_5OH_{anti}$	0.0	0.0	0.0	0.0	0.0	0.0	0.0	0.0	0.0	0.0	0.0	0.0	0.0
$Al^+ + C_2H_5OH_{gauche}$	−0.1	0.1	0.0	0.1	0.2	0.1	0.1	−0.3	−0.4	0.6	−0.1	−0.3	−0.5
$Al(C_2H_5OH)^+$ (**1a**)	−36.0	−34.6	−35.4	−35.6	−36.1	−36.9	−37.1	−39.3	−40.5	−36.2	−37.0	−39.2	−39.9
$Al(C_2H_5OH)^+$ (**1b**)	−36.5	−35.6	−36.5	−36.2	−37.0	−38.1	−37.7	−40.5	−41.3	−37.0	−37.7	−40.2	−40.8
TS 1/2	−0.2	−4.9	−9.7	−4.2	−3.7	−8.9	−3.2	−5.0	−10.7	−5.6	−10.6	−4.1	−9.8
$C_2H_5-Al^+-OH$ (**2**)	−49.9	−48.4	−51.5	−51.6	−46.0	−49.3	−49.1	−46.1	−49.7	−49.0	−52.2	−43.9	−47.5
TS 2/3[a]	−12.8	−13.5	−18.1	−17.3	−8.2	−13.1	−12.0	−9.6	−15.2	−13.1	−18.2	−6.8	−12.3
$(C_2H_4)Al^+(H)(OH)$ (**3**)	−42.6	−40.7	−42.2	−42.0	−36.3	−38.2	−37.7	−38.1	−40.8	−40.6	−42.4	−35.3	−37.9
TS 3/4	23.1	20.1	11.0	18.6	23.5	14.0	22.2	22.0	12.0	19.6	10.2	21.5	11.7
$(C_2H_4)Al^+(H_2O)$ (**4a**)	−26.2	−27.4	−27.8	−25.8	−25.8	−26.2	−24.1	−26.8	−27.7	−29.2	−29.7	−29.8	−30.4
$(C_2H_4)Al^+(H_2O)$ (**4b**)	−24.7	−25.1	−26.7	−24.6	−23.7	−25.2	−23.0	−24.6	−26.8	−27.0	−28.8	−27.8	−29.5
TS 2/4	5.0	−0.5	−4.5	0.0	0.9	−3.4	1.4	−0.1	−5.0	−1.2	−5.8	−0.4	−5.6
TS 1/4	−0.1	−2.3	−4.4	−4.6	−1.7	−3.9	−0.6	−3.3	−6.1	−3.4	−5.6	−4.5	−7.3
$Al(C_2H_4)^+ + H_2O$	−3.2	−5.4	−7.4	−4.6	0.4	−1.4	1.5	2.1	−0.2	−4.0	−6.3	0.3	−1.8
$Al(H_2O)^+ + C_2H_4$	−15.7	−17.7	−17.6	−15.7	−16.4	−16.4	−14.5	−14.8	−15.7	−19.4	−19.5	−19.2	−22.4
$Al^+ + H_2O + C_2H_4$	10.3	8.2	8.7	11.0	13.7	14.3	16.5	18.6	18.4	9.9	10.2	15.1	15.2

[a] In the case of the BPW91 and B3PW91 functionals, another conformer was found characterized by a lower relative energy of less than 5%.

kcal/mol. The dissociation energy for ethanol to water and ethylene *without* any aluminum ions is +10.3 and +8.7 kcal/mol for G2 and BPW91, respectively. As a result, the two ca. 2 kcal/mol differences add up to a difference between G2 and BPW91 of 4.2 kcal/mol.

Considering the transition-state energies calculated by different methods, the following can be noted. Similar to previous results,[43,44] the DFT and DFT/HF-hybrid methods have been found to underestimate reaction barriers also in the [Al^+,C_2H_5OH] system. The G2(QCI)[41] and G2 data are essentially the same. The B3LYP- and B3PW91-calculated relative energies of the transition states deviate by 2−5 kcal/mol from the G2 values. A difference of up to 10 kcal/mol can appear between the BPW91 and the G2 values.[43c,d] These findings suggest the use of the BPW91 or B3PW91 functional for computing the relative energies of minimum structures but B3LYP or B3PW91 for those of transition states.[52]

Recently, *base*-induced elimination reactions have been studied by means of DFT methods.[53] A strong basis-set dependence concerning the localization of transition states has been reported. The TS-characteristic large charge inhomogeneities and/or the inadequate description of the exchange interaction were held responsible. However, the present results on the *electrophile*-induced elimination did not support these findings.[53]

3.6. The E_{E2} Mechanism: Restricted to Gas-Phase Processes? According to the data presented in sections 3.2−3.4, the gas-phase reaction of Al^+ proceeds in a one-step manner via a single cyclic transition state (**TS 1/4**, see section 3.4). A reaction pathway via oxidative addition, β-H shift, and reductive elimination (see section 3.2, Figure 2 and Scheme 4) or via oxidative addition and 1,4-H shift (see section 3.3, Figure 3 and Scheme 5) is energetically more demanding. However, the differences are small in the decisive barrier heights, favoring **TS 1/4** vs **TS 2/4** (Table 2). They are ca. 1 (B3PW91) to 5 kcal/mol [G1, G2, G2(MP2, G2(QCI)]. The results of the BPW91 functionals however, provide an exception: The relative energy of **TS 2/4** is below that of **TS 1/4** when using 6-311++G(3df,2p) and cc-pVTZ basis sets by 0.1 and 0.2 kcal/mol, respectively. In any case, the syn-elimination product is formed. In comparison to the uncatalyzed process, $C_2H_5OH \rightarrow C_2H_4 + H_2O$, the aluminum cation reduces the reaction barrier by about 60 kcal/mol.

The present results on the Al^+ (^1S)-induced elimination of ethylene from ethanol indicate a new elimination reaction mechanism in the gas phase. It can be termed E_{E2}, because an elimination (E) takes place which is induced by an electrophile (E_E) and which follows second-order kinetics (E_{E2}). This mechanism is conceptually different from the textbook β-elimination mechanisms[54] E_1 and E_2. In the latter case, a base (B) influences the elimination as follows. It attacks the acidic hydrogen atom (E_{2H} in Scheme 7) or, to a certain degree, the carbon atom bearing the leaving group X (E_{2C}).[55] Regardless, this contrasts with the E_{E2} mechanism, which is characterized by the complexation of a metal cation (M^+, an electrophilic species) to the leaving group X. Concomitantly, the hydrogen atom moves toward the heteroatom in a single step yielding ethylene and $M(XH)^+$.

SCHEME 7

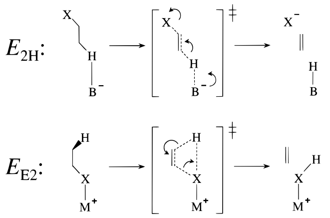

The E_{E2} scenario can be considered a mechanism for other experimental findings as well. For example in gas-phase chemistry, Eller and Schwarz introduced the *ion/dipole mechanism* for the elimination of HCN or HNC during the reaction of transition-metal ions with branched nitriles or isonitriles, respectively (Scheme 3).[22] But the intermediate ion/dipole complex can also rearrange according to the mechanism shown in Scheme 6. With regard to solution-phase chemistry, Mulzer and Black have independently reported on Lewis acid ($TiCl_4$, $AlBr_3$, $MgBr_2$, etc.) induced elimination reactions following *first-order kinetics*.[56]

4. Summary and Conclusion

The [Al^+,C_2H_5OH] PES has been explored using quantum chemistry methods. Post-Hartree−Fock and DFT methods have been applied to investigate the Al^+-induced ethylene elimination from ethanol. Reactants, products, intermediates, and transition states have been located. The character of each stationary point as a minimum or transition state was determined by the number of imaginary frequencies in a harmonic force-field calculation. Three distinct reaction pathways have been taken into account on the basis of experimental results:[10a,17] An oxidative-addition and reductive-elimination mechanism (section 3.2), an oxidative addition followed by a 1,4-H shift (section 3.3), and a new *electrophile*-induced one-step syn-elimination mechanism, E_{E2} (section 3.4) have been considered. The heights of the reaction barriers were determined for each process. The E_{E2} mechanism is energetically more favorable than the other pathways, but the decisive difference is only ca. 5 kcal/mol.

The DFT-computed relative energies of the minimum structures are comparable to those from G2 within ±5 kcal/mol. The DFT-predicted relative energies of the reaction barriers are lower than those of G2 (i) by 4−12 kcal/mol with BPW91 and (ii) by 2−5 kcal/mol with B3LYP and B3PW91. The basis set dependence of the DFT data is of minor importance if at least double-ζ quality basis sets were utilized.

Acknowledgment. The generous allocation of CPU time supplied by the Computer Group of the Max-Planck-Institut für Kohlenforschung in Mülheim a. d. Ruhr (MPI) and by the Gesellschaft für Wissenschaftliche Datenverarbeitung mbH Göttingen (GWDG) is acknowledged. We are grateful for the kind support provided by H. Lenk (MPI), O. Haan, J. Hattenbach, K. Heuer, and U. Schwardmann (GWDG). We thank J.-F. Gal for bringing ref 10b to our attention. We are grateful for the constructive comments by an anonymous referee.

Supporting Information Available: The molecular structures (*z* matrices) of complexes **1**−**4**, reactants, products, and transition states (15 pages). Ordering information is given on any current masthead page.

References and Notes

(1) Selected references: (a) Ziegler, K.; Holzkamp, E.; Breil, H.; Martin, H. *Angew. Chem.* **1955**, *67*, 541. (b) Natta, T. *Macromol. Chem.* **1955**, *16*, 213. (c) Sishta, S.; Hathorn, R. M.; Marks, T. J. *J. Am. Chem. Soc*. **1992**, *114*, 1112. (d) Pellececchia, C.; Grassi, A.; Immirzi, A. *J. Am. Chem. Soc.* **1994**, *116*, 1160 and references therein. (e) Fink, G., Mülhaupt, R., Brintzinger, H. H., Eds. *Ziegler Catalysts: Recent Scientific Innovations and Technological Improvements*; Springer-Verlag: Berlin, 1995.

(2) *Chem. Eng. News* **1993**, *71*, 1 (May 31), 27.

(3) (a) Coderman, R. C.; Beauchamp, J. L. *J. Am. Chem. Soc*. **1976**, *98*, 3998. (b) Freiser, B. S. *Chemtracts: Anal. Phys. Chem.* **1989**, *1*, 65. (c) Schwarz, J.; Schwarz, H. *Organometallics* **1994**, *13*, 1518. (d) Stöckigt, D.; Schwarz, J.; Schwarz, H. *J. Phys. Chem.* **1996**, *100*, 8786.

(4) (a) Ho, Y.-P.; Dunbar, R. C. Presented at the 43rd ASMS Conference on Mass Spectrometry and Allied Topics, Atlanta, GA, May 21−26, 1995. (b) Dunbar, R. C.; Klippenstein, S. J.; Hrušák, J.; Stöckigt, D.; Schwarz, H. *J. Am. Chem. Soc.* **1996**, *118*, 5277. (c) Klippenstein, S. J.; Yang, Y.-C.; Ryzhov, V.; Dunbar, R. C. *J. Chem. Phys.* **1996**, *104*, 4502.

(5) (a) Cassady, C. J.; Freiser, B. S. *J. Am. Chem. Soc.* **1984**, *106*, 6176. (b) Gobeli, D. A.; Yang, J. J.; El-Sayed, M. A. *Chem. Rev.* **1985**, *85*, 529. (c) van der Hart, W. J. *Mass Spectrom. Rev.* **1989**, *8*, 237. (d) Faulk, J. D.; Dunbar, R. C. *J. Am. Chem. Soc.* **1992**, *114*, 8596. (e) Lin, C. Y.; Dunbar, R. C. *J. Phys. Chem.* **1995**, *99*, 1754.

(6) (a) Ervin, K. M.; Armentrout, P. B. *J. Chem. Phys.* **1985**, *83*, 166. (b) Katritzky, A. R.; Watson, C. H.; Dega-Szafaran, Z.; Eyler, J. R. *J. Am. Chem. Soc.* **1990**, *112*, 2471. (c) Hop, C. E. C. A.; McMahon, T. B.; Willet, G. D. *Int. J. Mass Spectrom. Ion Processes* **1990**, *101*, 191. (d) Sunderlin, S. L.; Wang, D.; Squires, R. R. *J. Am. Chem. Soc.* **1993**, *115*, 12060. (e) Klassen, J. S.; Anderson, S. G.; Blades, A. T.; Kebarle, P. *J. Phys. Chem.* **1996**, *100*, 14218.

(7) (a) Lessen, D. E.; Asher, R. L.; Brucat, P. J. *J. Chem. Phys.* **1991**, *95*, 1414. (b) Willey, K. F.; Yeh, C. S.; Robbins, D. L.; Pilgrim, J. S.; Duncan, M. A. *J. Chem. Phys.* **1992**, *97*, 8886. (c) Duncan, M. A. *Annu. Rev. Phys. Chem.* **1997**, *48*, 69.

(8) (a) Stöckigt, D. *Chem. Phys. Lett.* **1996**, *250*, 387. (b) Stöckigt, D. *J. Phys. Chem.* **1997**, *101*, 3800.

(9) (a) Kappes, M. M.; Jones, R. W.; Staley, R. H. *J. Am. Chem. Soc.* **1982**, *104*, 888. (b) Kappes, M. M.; Staley, R. H. *J. Am. Chem. Soc.* **1982**, *104*, 1813. (c) Kappes, M. M.; Staley, R. H. *J. Am. Chem. Soc.* **1982**, *104*, 1819. (d) Jones, R. W.; Staley, R. H. *J. Am. Chem. Soc.* **1982**, *104*, 2296. (e) Operti, L.; Tews, E. C.; Freiser, B. S. *J. Am. Chem. Soc.* **1988**, *110*, 3847.

(10) (a) Uppal, J. S.; Staley, R. H. *J. Am. Chem. Soc.* **1982**, *104*, 1229, 1235. (b) Gal, J.-F.; Taft, R. W.; McIver, R. T., Jr. *Spectrosc. Int. J.* **1984**, *3*, 96.

(11) (a) Andrews, L., Moskovits, M., Eds. *Chemistry and Physics of Matrix-Isolated Species*; Elsevier: Amsterdam, 1989. (b) Freivogel, P.; Grutter, M.; Forney, D.; Maier, J. P. *Chem. Phys.* **1997**, *216*, 401. (c) Maier, G.; Reisenauer, H. P.; Preiss, T.; Pacl, H.; Jürgen, D.; Tross, R.; Senger, S. *Pure Appl. Chem.* **1997**, *69*, 113.

(12) (a) Russel, D. H., Ed. *Gas-Phase Inorganic Chemistry*; Plenum Press: New York, 1989. (b) Eller, K.; Schwarz, H. *Chem. Rev.* **1991**, *91*, 1121. (c) Armentrout, P. B. In *Selective Hydrocarbon Activation: Principles and Progress*; Davies, J. A., Watson, P. L., Liebman, J. F., Greenberg, A., Eds.; VCH: New York, 1990. (d) Weisshaar, J. C. *Acc. Chem. Res.* **1993**, *26*, 213. (e) Schröder, D.; Schwarz, H. *Angew. Chem., Int. Ed. Engl.* **1995**, *34*, 1973.

(13) For a few interesting examples, see: (a) Nagase, S.; Ray, N. K.; Morokuma, K. *J. Am. Chem. Soc.* **1980**, *102*, 4536. (b) Wang, X.; Li, Y.; Wu, Y.-D.; Paddon-Row, M. N.; Rondan, N. G.; Houk, K. N. *J. Org. Chem.* **1990**, *65*, 2601. (c) Bundens, J. W.; Francl, M. M. *Organometallics* **1993**, *12*, 1608.

(14) (a) Hrušák, J.; Stöckigt, D.; Schwarz, H. *Chem. Phys. Lett.* **1994**, *221*, 518. (b) Stöckigt, D.; Hrušák, J. *J. Phys. Chem.* **1994**, *98*, 3675. (c) Stöckigt, D.; Holthausen, M. C.; Koch, W.; Schwarz, H. *J. Phys. Chem.* **1995**, *99*, 5950. (d) Stöckigt, D.; Hrušák, J.; Schwarz, H. *Int. J. Mass Spectrom. Ion Processes* **1995**, *149/150*, 1.

(15) (a) Weller, T.; Meiler, W. *Chem. Phys. Lett.* **1983**, *98*, 541. (b) Smith, S. F.; Chandrsekhar, J.; Jorgensen, W. L. *J. Phys. Chem.* **1983**, *87*, 1898. (c) Balaji, V.; Sunil, K. K.; Jordan, K. D. *Chem. Phys. Lett.* **1987**, *136*, 309. (d) Srinivas, R.; Sülzle, D.; Schwarz, H. *J. Am. Chem. Soc.* **1990**, *112*, 8334. (e) Alcamí, M.; Mó, O.; Yáñez, M. *J. Mol. Struct. (THEOCHEM)* **1991**, *234*, 357. (f) Sodupe, M.; Bauschlicher, C. W., Jr. *Chem. Phys. Lett.* **1991**, *181*, 321. (g) Mó, O.; Yáñez, M.; Total, A.; Tortajada, J.; Morizur, J. P. *J. Phys. Chem.* **1993**, *97*, 5553. (h) Watanabe, H.; Iwata, S. *J. Phys. Chem.* **1996**, *100*, 3377.

(16) Chowdhury, A. K.; Wilkins, C. L. *Int. J. Mass Spectrom. Ion Processes* **1988**, *82*, 163.

(17) Bouchard, F.; Brenner, V.; Carra, C.; Hepburn, J. W.; Koyanagi, G. K.; McMahon, T. B.; Ohanessian, G.; Peschke, M. *J. Phys. Chem. A* **1997**, *101*, 5885.

(18) For a recent study of elimination reactions within Al(H$_2$O)$^+$ clusters, see: Beyer, M.; Berg, C.; Görlitzer, H. W.; Schindler, T.; Achatz, U.; Albert, G.; Niedner-Schatteburg, G.; Bondybey, V. E. *J. Am. Chem. Soc.* **1996**, *118*, 7386.

(19) (a) Elschenbroich, C.; Salzer, A. *Organometallics*; VCH Publishers: New York, 1989. (b) Crabtree, R. H. *The Organometallic Chemistry of the Transition Metals*; Wiley: New York, 1988. (c) Parshall, G. W. *Homogeneous Catalysis*; Wiley: New York, 1980.

(20) Tsuji, J. *Palladium Reagents and Catalysts: Innovations in Organic Synthesis*; Wiley: New York, 1995.

(21) (a) Herbst, E. *Astrophys. J.* **1987**, *313*, 867. (b) Herbst, E.; Smith, D.; Adams, N. G.; McIntosh, B. J. *J. Chem. Soc., Faraday Trans. 2* **1989**, *85*, 1655. (c) Meot-Ner (Mautner), M.; Sieck, L. W. *Int. J. Mass Spectrom. Ion Processes* **1989**, *92*, 123. (d) Bouchoux, G.; Hopillard, Y. *J. Am. Chem. Soc.* **1990**, *112*, 9110. (e) Swanton, D. J.; Marsden, C. J.; Radom, L. *Org. Mass Spectrom.* **1991**, *26*, 228. (f) Radom, L. *Int. J. Mass Spectrom. Ion Processes* **1992**, *118/119*, 339. (g) Mason, R. S.; Parry, A. *Int. J. Mass Spectrom. Ion Processes* **1994**, *133*, 47. (h) Karpas, Z.; Eiceman, G. A.; Ewing, R. G.; Harden, C. S. *Int. J. Mass Spectrom. Ion Processes* **1994**, *133*, 47. (i) Audier, H. E.; Koyannagi, G. K.; McMahon, T. B.; Thölmann, D. *J. Phys. Chem. A* **1996**, *100*, 8220. (j) Matthews, K. K.; Adams, N. G.; Fisher, N. D. *J. Phys. Chem. A* **1997**, *101*, 2841. (k) Fairley, D. A.; Scott, G. B. I.; Freeman, C. G.; Maclagan, R. G. A. R.; McEwan, M. J. *J. Phys. Chem. A* **1997**, *101*, 2848.

(22) (a) Eller, K.; Schwarz, H. *Chimia* **1989**, *43*, 371. (b) Eller, K.; Schwarz, H. *Organometallics* **1989**, *8*, 1820. (c) Eller, K.; Karrass, S.; Schwarz, H. *Ber. Bunsen-Ges. Phys. Chem.* **1990**, *94*, 1201. (d) Eller, K.; Zummack, W.; Schwarz, H. *J. Am. Chem. Soc.* **1990**, *112*, 621.

(23) For examples of *multiplet* transition-metal systems, see: (a) Schwarz, J.; Heinemann, C.; Schwarz, H. *J. Phys. Chem.* **1995**, *99*, 11405. (b) Heinemann, C.; Schwarz, J.; Koch, W.; Schwarz, H. *J. Chem. Phys.* **1995**, *103*, 4551. (c) Heinemann, C.; Schwarz, J.; Schwarz, H. *J. Phys. Chem.* **1996**, *100*, 6088.

(24) (a) Tortajada, J.; Total, A.; Morizur, J. P.; Alcamí, M.; Mó, M.; Yáñez, M. *J. Phys. Chem.* **1992**, *96*, 8309. (b) Mó, O.; Yáñez, M.; Total, A.; Tortajada, J.; Morizur, J. P. *J. Phys. Chem.* **1993**, *97*, 5553. (c) Kemper, P. R.; Bushnell, J.; Bowers, M. T.; Gellene, G. I. *J. Phys. Chem.* **1998**, *A102*, 8590. (d) Dunbar, R. C. *J. Phys. Chem.* **1998**, *A102*, 8946.

(25) Frisch, M. J.; Trucks, G. W.; Schlegel, H. B.; Gill, P. M. W.; Johnson, B. G.; Robb, M. A.; Cheeseman, J. R.; Keith, T.; Petersson, G. A.; Montgomery, J. A.; Raghavachari, K.; Al-Laham, M. A.; Zakrzewski, V. G.; Ortiz, J. V.; Foresman, J. B.; Peng, C. Y.; Ayala, P. Y.; Chen, W.; Wong, M. W.; Andres, J. L.; Replogle, E. S.; Gomperts, R.; Martin, R. L.; Fox, D. J.; Binkley, J. S.; Defrees, D. J.; Baker, J.; Stewart, J. P.; Head-

Gordon, M.; Gonzalez, C.; Pople, J. A. *Gaussian 94*, Revision B.3; Gaussian, Inc.: Pittsburgh, PA, 1995.

(26) Ziegler, T. *Chem. Rev.* **1991**, *91*, 651.

(27) March, N. H. *Electron Density Theory of Atoms and Molecules*; Academic Press: London, 1992.

(28) Tschinke, V.; Ziegler, T. *Theor. Chim. Acta* **1991**, *81*, 651.

(29) (a) Vosko, S. H.; Wilk, L.; Nusair, M. *Can. J. Phys.* **1980**, *58*, 1200 and references therein. (b) Colle, R.; Salvetti, O. *J. Chem. Phys.* **1983**, *79*, 1404. (c) Perdew, J. P. *Phys. Rev. B* **1986**, *33*, 8822. (d) Lee, C.; Yang, W.; Parr, R. G. *Phys. Rev. B* **1988**, *37*, 785. (e) Becke, A. D. *J. Chem. Phys.* **1988**, *88*, 1053. (f) Becke, A. D. *Phys. Rev. A* **1988**, *38*, 3098. (g) Perdew, J. P.; Wang, Y. *Phys. Rev. B* **1992**, *45*, 13244. (h) Baker, J.; Muir, M.; Andzelm, J. *J. Chem. Phys.* **1995**, *102*, 2063. (i) Becke, A. D. *J. Chem. Phys.* **1996**, *104*, 1040.

(30) Curtiss, L. A.; Raghavachari, K.; Trucks, G. W.; Pople, J. A. *J. Chem. Phys.* **1991**, *94*, 7221.

(31) Becke, A. D. *J. Chem. Phys.* **1993**, *98*, 5648.

(32) (a) Becke, A. D. *J. Chem. Phys.* **1988**, *88*, 2547. (b) Stephens, P. J.; Devlin, F. J.; Chabalowski, C. F.; Frisch, M. J. *J. Phys. Chem.* **1994**, *98*, 11623.

(33) (a) Barone, V. *Chem. Phys. Lett.* **1994**, *226*, 392. (b) Martin, J. M. L.; El-Yazal, J.; Francois, J.-P. *Mol. Phys.* **1995**, *86*, 1437. (c) Barone, V.; Adamo, C.; Mele, F. *Chem. Phys. Lett.* **1996**, *249*, 290. (d) Jacobsen, H.; Ziegler, T. *Inorg. Chem.* **1996**, *35*, 775. (e) Vanquickenborne, L. G.; Vinckier, A. E.; Pierloot, K. *Inorg. Chem.* **1996**, *35*, 1305. (f) Lopez, X.; Ugalde, J. M.; Cossio, F. P. *J. Am. Chem. Soc.* **1996**, *118*, 2718. (g) Margl, P.; Lohrenz, J. C. W.; Ziegler, T.; Blöchl, P. E. *J. Am. Chem. Soc.* **1996**, *118*, 4434. (h) Goldstein, E.; Beno, B.; Houk, K. N. *J. Am. Chem. Soc.* **1996**, *118*, 6036. (i) Problems have been reported in applying DFT, see: Sulzbach, H. M.; Schaefer, H. F., III. *J. Am. Chem. Soc.* **1996**, *118*, 3519.

(34) Laming, G. J.; Termath, V.; Handy, N. C. *J. Chem. Phys.* **1993**, *99*, 5612.

(35) (a) Krishnan, R.; Binkley, J. S.; Seeger, R.; Pople, J. A. *J. Chem. Phys.* **1980**, *72*, 650. (b) Guo, H.; Karplus, M. *J. Chem. Phys.* **1989**, *91*, 1719.

(36) (a) Woon, D. E.; Dunning, T. H., Jr. *J. Chem. Phys.* **1993**, *98*, 1358. (b) Woon, D. E.; Dunning, T. H., Jr. *J. Chem. Phys.* **1994**, *100*, 2975 and references therein.

(37) Basis sets were obtained in part from the Extensible Computational Chemistry Environment Basis Set Database, version 1.0, as developed and distributed by the Molecular Science Computing Facility, Environmental and Molecular Sciences Laboratory, which is part of the Pacific Northwest Laboratory, P.O. Box 999, Richland, WA 99352, and funded by the U.S. Department of Energy (http://www.emsl.pnl.gov:2080/forms/basisform.html). The Pacific Northwest Laboratory is a multiprogram laboratory operated by Battelle Memorial Institute for the U.S. Department of Energy under Contract DE-AC06-76RLO 1830. Contact David Feller, Karen Schuchardt, or Don Jones for further information.

(38) The DFT-computed imaginary frequencies of the transition states differ from the MP2-computed ones as follows: **TS 1/2** − B3LYP/6-311+G(d) *i*276 cm−1, BPW91/6-311+G(d) *i*289 cm^{-1}, B3PW91/6-311+G(d) *i*308 cm^{-1}, MP2(full)/6-31G(d) *i*436 cm^{-1}; **TS 2/3** − B3LYP/6-311+G(d) *i*785 cm^{-1}, BPW91/6-311+G(d) *i*695 cm^{-1}, B3PW91/6-311+G(d) *i*751 cm^{-1}, MP2(full)/6-31G(d) *i*995 cm^{-1}; **TS 3/4** − B3LYP/6-311+G(d) *i*1358 cm^{-1}, BPW91/6-311+G(d) *i*1226 cm^{-1}, B3PW91/6-311+G(d) *i*1358 cm^{-1}, MP2(full)/6-31G(d) *i*1273 cm^{-1}; **TS 2/4** − B3LYP/6-311+G(d) *i*399 cm^{-1}, BPW91/6-311+G(d) *i*502 cm^{-1}, B3PW91/6-311+G(d) *i*441 cm^{-1}, MP2(full)/6-31G(d) *i*430 cm^{-1}; **TS 1/4** − B3LYP/6-311+G(d) *i*664 cm^{-1}, BPW91/6-311+G(d) *i*786 cm^{-1}, B3PW91/6-311+G(d) *i*679 cm^{-1}, MP2(full)/6-31G(d) *i*646 cm^{-1}.

(39) (a) Gonzales, C.; Schlegel, H. B. *J. Chem. Phys.* **1989**, *90*, 2154. (b) Gonzales, C.; Schlegel, H. B. *J. Phys. Chem.* **1990**, *94*, 5523. (c) Deng, L.; Ziegler, T. *Int. J. Quantum Chem.* **1994**, *52*, 731.

(40) Møller, C.; Plesset, M. S. *Phys. Rev.* **1934**, *46*, 618.

(41) Curtiss, L. A.; Carpenter, J. E.; Raghavachari, K.; Pople, J. A. *J. Chem. Phys.* **1992**, *96*, 9030.

(42) Different computer codes have been tested for their accuracy in DFT calculations: Kotochigova, S.; Levine, Z.; Shirley, E.; Stiles, M.; Clark, C. *Atomic Reference Data for Electronic Structure Calculations*, http://math.nist.gov/DFTdata/atomdata/narrative.html. (Nov. 16 1998).

(43) (a) Fan, L.; Ziegler, T. *J. Chem. Phys.* **1990**, *92*, 3645. (b) Stanton, R. V.; Merz, K. M., Jr. *J. Chem. Phys.* **1994**, *100*, 434. (c) Baker, J.; Andzelm, J.; Muir, M.; Taylor, P. R. *Chem. Phys. Lett.* **1995**, *237*, 53. (d) Baker, J.; Muir, M.; Andzelm, J. *J. Chem. Phys.* **1995**, *102*, 2063. (e) Nguyen, M. T.; Creve, S.; Vanquickenborne, L. G. *J. Phys. Chem.* **1996**, *100*, 18422. (f) Jursic, B. S. *Chem. Phys. Lett.* **1996**, *156*, 213. (g) Basch, H.; Hoz, S. *J. Phys. Chem. A* **1997**, *101*, 4416.

(44) (a) Margl, P.; Ziegler, T.; Blöchl, P. E. *J. Am. Chem. Soc.* **1995**, *117*, 12625. (b) Torrent, M.; Deng, L.; Duran, M.; Sola, M.; Ziegler, T. *Organometallics* **1997**, *16*, 13. (c) Deng, Q.; Thomas, B. E., IV; Houk, K. N.; Dowd, P. *J. Am. Chem. Soc.* **1997**, *119*, 6902. (d) Cunje, A.; Rodriquez, C. F.; Bohme, D. K.; Hopkinson, A. C. *J. Phys. Chem. A* **1998**, *102*, 478.

(45) (a) Through the use of the 6-311+G(d) basis set, the geometrical data from BPW91, B3PW91, B3LYP, and MP2 calculations of each minimum were found to be similar within less than 1% (bond lengths and angles), with a few exceptions. (b) For detailed geometrical parameters, see the *z* matrices in the Supporting Information.

(46) (a) Durig, J. R.; Bucy, W. E.; Wurrey, C. J.; Carreira, L. A. *J. Phys. Chem.* **1975**, *79*, 988. (b) St.-Amant, A.; Cornell, W. D.; Kollman, P. A.; Halgren, T. A. *J. Comput. Chem.* **1995**, *16*, 1483.

(47) Oie, T.; Topol, I. A.; Burt, S. K. *J. Phys. Chem.* **1995**, *99*, 905.

(48) For selected excellent studies on β-H shifts in organometallic systems, see: (a) Versluis, L.; Ziegler, T. *J. Am. Chem. Soc.* **1990**, *112*, 6763. (b) Blum, O.; Milstein, D. *J. Am. Soc. Chem.* **1995**, *117*, 4582. (c) Fiedler, A.; Schröder, D.; Schwarz, H.; Tjelta, B. L.; Armentrout, P. B. *J. Am. Chem. Soc.* **1996**, *118*, 5047.

(49) (a) Siegbahn, P. E. M.; Blomberg, M. R. A.; Svensson, M. *J. Phys. Chem.* **1993**, *97*, 2564. (b) Siegbahn, P. E. M.; Blomberg, M. R. A.; Svensson, M. *J. Am. Chem. Soc.* **1993**, *115*, 1952. (c) Blomberg, M. R. A.; Siegbahn, P. E. M.; Svensson, M. *Inorg. Chem.* **1993**, *32*, 4218. (d) Siegbahn, P. E. M.; Blomberg, M. R. A.; Svensson, M. *J. Am. Chem. Soc.* **1993**, *115*, 4191.

(50) Stöckigt, D. Unpublished results. These data were obtained with B3PW91/6-311++G(3df,2p)//B3PW91/6-311+G(d).

(51) Weitzel, K. M. *Chem. Phys. Lett.* **1991**, *186*, 490.

(52) However, the B3LYP functional underestimates $D_0[\mathrm{Al}^+-(\pi\text{-L})]$ by ca. 5 kcal/mol independent of the applied basis set (π-L: benzene, cyclopentadiene, furane, and pyrrole). This contrasts the findings with the BPW91 and B3PW91 functionals (cf. ref 8b).

(53) (a) Bickelhaupt, F. M.; Nibbering, N. M. M.; Baerends, E. J.; Ziegler, T. *J. Am. Chem. Soc.* **1993**, *115*, 9160. (b) Gronert, S.; Merrill, G. N.; Kass, S. R. *J. Org. Chem.* **1995**, *60*, 488. (c) Bickelhaupt, F. M.; Baerends, E. J.; Nibbering, N. M. M. *Chem. Eur. J.* **1996**, *2*, 196. (d) Merrill, G. N.; Gronert, S.; Kass, S. R. *J. Phys. Chem. A* **1997**, *101*, 208.

(54) (a) Morrison, R. T.; Boyd, R. N. *Organic Chemistry*, 4th ed.; Allyn and Bacon: Boston, 1983. (b) March, J. *Advanced Organic Chemistry*, 4th ed.; Wiley: New York, 1992.

(55) (a) Parker, A. J.; Ruane, M.; Biale, G.; Winstein, S. *Tetrahedron Lett.* **1968**, *17*, 2113. (b) Ko, E. C. F.; Parker, A. J. *J. Am. Chem. Soc.* **1968**, *90*, 6447.

(56) (a) Mulzer, J.; Pointner, A.; Strasser, R.; Hoyer, K.; Nagel, U. *Tetrahedron Lett.* **1995**, *36*, 3679. (b) Black, T. H.; McDermott, T. S. *J. Chem. Soc., Chem. Commun.* **1991**, 184. (c) Banthrope has coined the term "specific electrophilic catalysis" for Ag$^+$- or Hg^{2+}-induced E_1 reactions from organic halides: Banthrope, D. V. Elimination Reactions. In *Reaction Mechanisms in Organic Chemistry*; Hughes, E. D., Ed.; Elsevier: Amsterdam, 1963.